

## Composition Dependent Optical Properties of Vacuum Deposited $Sb_{2x}Bi_{2(1-x)}Te_3$ Thin Films for Thermoelectric Applications

\*<sup>1</sup> G.D. Deshmukh

\*<sup>1</sup> Associate Professor, Department of Physics, Nana Saheb Y.N. Chavan Arts, Science and Commerce College, Chalisgaon, Jalgaon, Maharashtra, India.

### Article Info.

E-ISSN: 2583-6528

Impact Factor (SJIF): 6.876

Peer Reviewed Journal

Available online:

[www.alladvancejournal.com](http://www.alladvancejournal.com)

Received: 28/Nov/2024

Accepted: 26/Dec/2024

### Abstract

The ternary thin films  $Sb_{2x}Bi_{2(1-x)}Te_3$ , a class of group V-VI materials were deposited via sublimation by thermal evaporation in vacuum. These materials are known for their thermoelectric and topological insulating properties. The systematic exploration of  $Sb_2Te_3$ - $Bi_2Te_3$  alloys, achieved by tuning antimony concentrations, reveals significant manipulation of their electronic band structure and their optical response. The films are polycrystalline exhibiting rhombohedral or hexagonal structure. The grain size observed about 20-60 nm. Optical transmittance spectra show optical transparency in the spectral region between 1100 nm to 2500 nm, between 0% to 32% corresponding to the composition. The optical reflectance varies from 12% to 70 % and increases with increase in the composition. The optical band gap has been found to be direct and allowed, it vary between 0.92 eV to 1.06 eV with composition. Refractive index diverges from 1.58 to 8.42 and extinction coefficient varies from 0.42 to 3.02 for all the compositions.

### \*Corresponding Author

G.D. Deshmukh

Associate Professor, Department of Physics, Nana Saheb Y.N. Chavan Arts, Science and Commerce College, Chalisgaon, Jalgaon, Maharashtra, India.

**Keywords:** Thermal evaporation, thermoelectric, transmittance, band gap, refractive index, extinction coefficient

### Introduction

The investigation of novel materials with tunable optical characteristics is crucial for advancing optoelectronic devices, with topological insulators garnering significant attention due to their unique surface states. Particularly  $Bi_2Te_3$ , have emerged as prominent candidate due to its robust topological properties and narrow band gaps, making them suitable for infrared photo detection and thermoelectric [1]. The incorporation of Sb into the  $Bi_2Te_3$  lattice, forming  $Sb_{2x}Bi_{2(1-x)}Te_3$  alloys, offers a promising route to manipulate their electronic band structure and consequently, their optical response. This alloying strategy allows for precise control over the material's properties by tuning the antimony concentration, leading to optimized performance in various optical applications [2]. A systematic study of the band structure evolution and its correlation with observed optical phenomena, providing a pathway to engineer materials with targeted optoelectronic responses [3]. This systematic investigation into the optical properties of  $Sb_{2x}Bi_{2(1-x)}Te_3$  thin films aims to provide a broad understanding of their suitability for various optoelectronic applications, including

displays, solid-state lighting, and lasing [4]. The ability to engineer the optoelectronic properties of these materials through precise control of composition opens up possibilities for their use in high-efficiency solar cells and advanced thermoelectric devices [5]. These binary and ternary compounds also find applications in electronics, optoelectronics, microelectronics, thermal sensor, wide-band radiation detectors and electromechanical devices [6]. Nanostructured  $Sb_2Te_3$ / $Bi_2Te_3$  materials have been extensively investigated by theoretical and experimental researchers recently. It has been found that nanoengineering of thermoelectric materials could result in higher value of figure of merit. They are semi-metal alloy and have good electrical conductivity [7]. Chalcogenide glasses are sensitive to the absorption of electromagnetic radiation and show a variety of photo-induced effects. These glasses offer potential use in photo-resist, microelectronic, optoelectronic, holographic applications and particularly their ability to transmit light in the mid to far-infrared region. Chalcogenide glasses are the most capable materials for a wider range of wavelengths, near and mid-infrared [8,9,10].

## Experimental

Using  $\text{Sb}_2\text{Te}_3$  and  $\text{Bi}_2\text{Te}_3$  powder (Sigma-Aldrich 99.99+ % purity) the ternary thin films of  $\text{Sb}_{2x}\text{Bi}_{2(1-x)}\text{Te}_3$  ( $x = 0.1$  to  $0.9$ ) were deposited via sublimation of the compound onto well cleaned glass substrates by thermal evaporation in vacuum ( $\approx 10^{-5}$  torr) using molybdenum boat as a source. For the preparation of ternary semiconductors of  $\text{Sb}_{2x}\text{Bi}_{2(1-x)}\text{Te}_3$  ( $x = 0.1$  to  $0.9$ ) the constituent compounds of  $\text{Sb}_2\text{Te}_3$  and  $\text{Bi}_2\text{Te}_3$  have been taken in molecular stoichiometry proportional weights, crushed and mixed homogenously. The different sets of samples having varying compositions ( $x = 0.1$  to  $0.9$ ) with different thicknesses for the ternaries were deposited under controlled and similar growth conditions. The rate of deposition and thickness of the films were controlled by using quartz crystal thickness monitor model DTM-101 provided by HINDHIVAC. The deposition rate was maintained 3–5 Å/sec constant throughout the sample preparations. The source to substrate distance was kept constant (14 cm). The radiation from the red hot boat raised temperature of the substrate by 6–8 K depending on the boat temperature during the deposition process. Deposited samples were kept under vacuum overnight. The selected samples of  $\text{Sb}_{2x}\text{Bi}_{2(1-x)}\text{Te}_3$  ( $x = 0.1$  to  $0.9$ ) thin films with nearly equal thicknesses ( $\approx 2500$  Å) were used for the study. Adequate subsequent heat treatment is expected to remove the defects and to improve the electrical and thermoelectric properties. Therefore these samples were annealed at 473 K for 1 hour in vacuum ( $\approx 10^{-5}$  torr) and used for the characterization.

## Result and Discussion

### Characterization

The X-ray diffraction patterns of selected  $\text{Sb}_{2x}\text{Bi}_{2(1-x)}\text{Te}_3$

annealed samples were recorded by X-ray diffractometer (Bruker, model D-8 Advance) with  $\text{CuK}\alpha$  radiation (1.5406 Å). The surface morphology of these films was investigated by field emission scanning electron microscope (FESEM) using model Hitachi S-4800-II (Japan). Quantitative elemental analysis of the films was carried out by computer controlled energy dispersive X-ray analyzer (EDAX) attached to the field emission scanning electron microscope. The transmittance  $T(\lambda)$  and reflectance  $R(\lambda)$  of the films were measured in the spectral range of 200–2500 nm, using the model JASCO V-670 UV–VIS–NIR double beam spectrophotometer.

### Structural Characterization

The XRD patterns of the thermally evaporated  $\text{Sb}_{2x}\text{Bi}_{2(1-x)}\text{Te}_3$  ( $x = 0.1$  to  $0.9$ ) thin films of thickness 2500 Å annealed at 473 K for 1 hour in vacuum are shown in Fig. 1(a) to (c). It shows that, all the films are polycrystalline exhibiting rhombohedral structure. Crystals in the rhombohedral system can be referred to either a rhombohedral or a hexagonal lattice [11]. The patterns show strong preferential orientation of the crystallites along (1010) direction for all the compositions. In all cases these samples also shows lower intensity peak for (110) and very low intensity peaks for (118) and (300) planes of hexagonal or rhombohedral phase corresponding to different compositions. K. Rajasekar *et al* [12] reported analogous orientation of the crystals. Thus these ternary composite films with different compositions are having rhombohedral or hexagonal crystal structures confirmed by using JCPDS X-ray powder file data of  $\text{Sb}_2\text{Te}_3$  (15-0874) and  $\text{Bi}_2\text{Te}_3$  (15-0863).

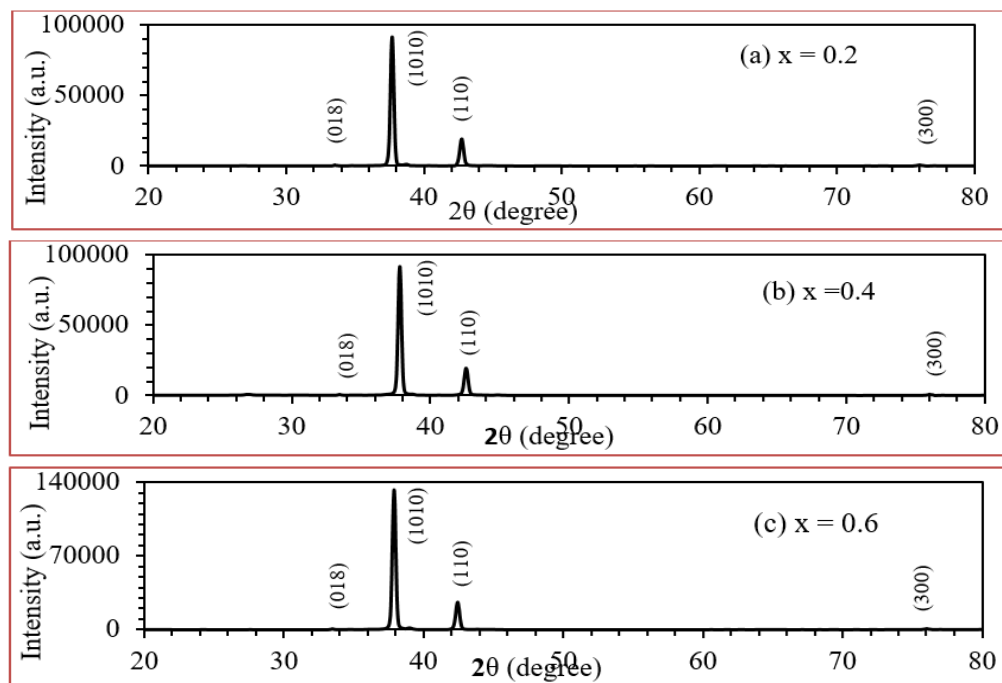


Fig 1: XRD patterns of  $\text{Sb}_{2x}\text{Bi}_{2(1-x)}\text{Te}_3$  thin films annealed at 473 K for 1 hour in vacuum

### FESEM Analysis

The field emission scanning electron microscope (FESEM) images of  $\text{Sb}_{2x}\text{Bi}_{2(1-x)}\text{Te}_3$  thin films of different compositions annealed at 473 K for 1 hour in vacuum ( $\approx 10^{-5}$  torr) are shown in Fig. 2. For all the compositions the FESEM micrographs are analyzed at a resolution of 300nm with 150K

X magnification, having an accelerating voltage of 15 kV. The images show that the deposited films are polycrystalline in nature with homogeneous surface, uniform deposition and crack free. All films show good crystallinity. The grains are found to be nano size and closely packed with less inter grain spacing.

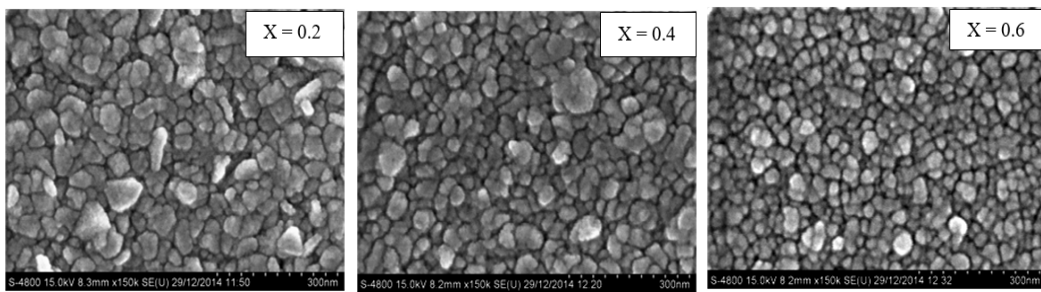


Fig 2: FESEM micrographs of annealed Sb<sub>2x</sub>Bi<sub>2(1-x)</sub>Te<sub>3</sub> films of different compositions

### Optical Analysis

The reflectance and transmittance spectra of Sb<sub>2x</sub>Bi<sub>2(1-x)</sub>Te<sub>3</sub> samples were recorded using JASCO V-670 UV-VIS-NIR double beam spectrophotometer in the spectral range of 200–2500 nm. The optical Transmittance (%) T and Reflectance (%) R spectra of these thin films annealed at 473 K for 1 hour in vacuum, in the wavelength range 200–2500 nm are shown in Fig. 3 and Fig. 4 respectively. For all the films, spectra reveal absence of interference effects for wavelength away

from the fundamental absorption edge. High transmittance in a higher wavelength region and a sharp absorption edge were observed in the films. All the samples ( $x = 0.1$  to  $0.9$ ) show optical transparency in the spectral region between 1100 nm to 2500 nm and display a clear explicit absorption edge interrelated to the optical band gap depending on the composition of the films. It is observed that the transmittance falls steeply with decreasing wavelength.

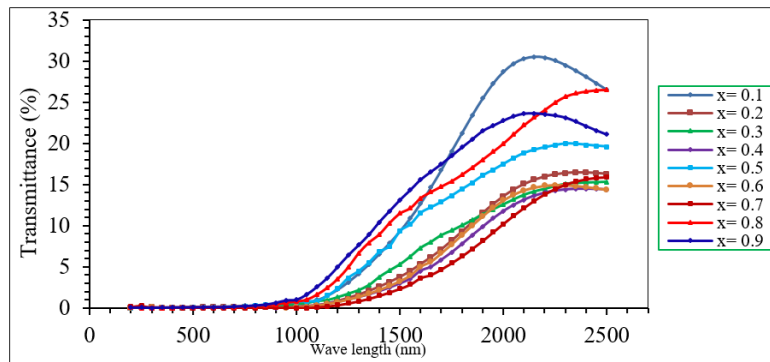


Fig 3: Transmittance spectra of annealed Sb<sub>2x</sub>Bi<sub>2(1-x)</sub>Te<sub>3</sub> thin films

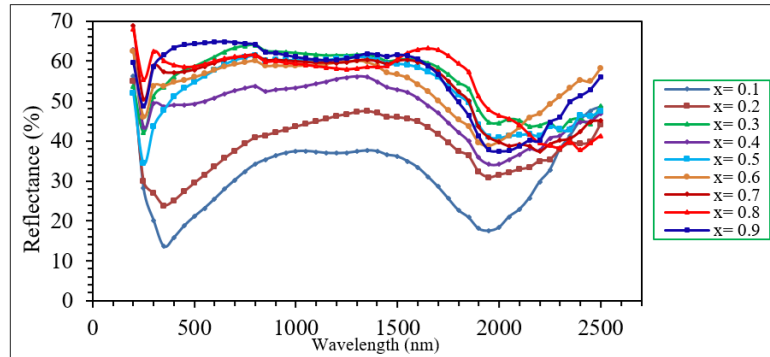


Fig 4: Reflectance spectra of annealed Sb<sub>2x</sub>Bi<sub>2(1-x)</sub>Te<sub>3</sub> thin films

The films with composition  $x = 0.1$  to  $0.9$  shows distinct optical transmittance between 0 % to 32 %. With the increase in  $x$  from 0.1 to 0.7 i.e. increasing the composition of Sb<sub>2</sub>Te<sub>3</sub> in to the film, the absorption edge shifts towards higher wavelength region, where as for the compositions  $x = 0.8$  and  $0.9$  the edge shifts towards lower wavelength region. Depending on the composition, considerable absorption is observed throughout the wavelength region 200–1100 nm. The maxima and minima due to interference effects obtained as in case of Bi<sub>2</sub>Te<sub>3</sub><sub>x</sub>Se<sub>3(1-x)</sub> thin films are not observed in these Sb<sub>2x</sub>Bi<sub>2(1-x)</sub>Te<sub>3</sub> thin films. For all the compositions the reflectance varies from 12% to 70 %, it increases with increase in the composition. Absorption coefficients ( $\alpha$ ) have been evaluated using percentage transmittance data and following equation

$$\alpha = \frac{2.303}{d} \log_{10} \left( \frac{1}{T} \right) \quad (1)$$

The absorption coefficient can be written in general form as a function of incident photon energy  $h\nu$  as

$$\alpha h\nu = A (h\nu - E_g)^P \quad (2)$$

where  $E_g$  is the optical band gap, A is a constant and  $P$  has discrete values like 1/2, 3/2, 2 or more depending on whether the transition is direct or indirect, and allowed or forbidden. In the direct and allowed cases  $P = 1/2$ , whereas for the direct but forbidden cases it is 3/2. But for the indirect and allowed case  $P = 2$  and for the forbidden cases it will be 3 or more.

The value of  $P$  determines the nature of optical transition. The results have been analyzed according to relation (2). The plot of  $(\alpha h\nu)^2$  versus  $h\nu$  for these annealed films is presented in Fig. 5 (a) to (i). These figure shows clearly the linear dependence for the value of  $P=1/2$ . This is attributed to an allowed and direct transition with direct band gap energies. The lattice parameter ( $a$ ) varies almost linearly and decreases continuously with increase in composition ( $x$ ). Fig. 6 also shows that at the lower composition ( $x = 0.1$  to 0.7) the optical band gap ( $E_g$ ) increases linearly from 0.92 eV to 1.06 eV, whereas at the higher composition ( $x = 0.8$  and 0.9) it decreases. K. Sharma *et al.* [13] reported that for the

$(\text{Bi}_2\text{Te}_3)_x(\text{Sb}_2\text{Te}_3)_{1-x}$  alloy, optical band gap decreased with increase in the Sb content and the observed band gap shrinkage is dependent on the carrier concentration thus resulting in narrowing band gap effect. Nidhi Jain *et al.* [9] concluded that values of band gap increases from 0.83 eV to 1.25 eV with decrease in concentration of Bi from 20 to 4 at % for the Se-Sb-Bi glassy alloys. The optical band gap is a bond sensitive property [14]. Not many theoretical and experimental investigations have focused on the band gap versus composition properties of ternary  $\text{Sb}_{2x}\text{Bi}_{2(1-x)}\text{Te}_3$  thin films.

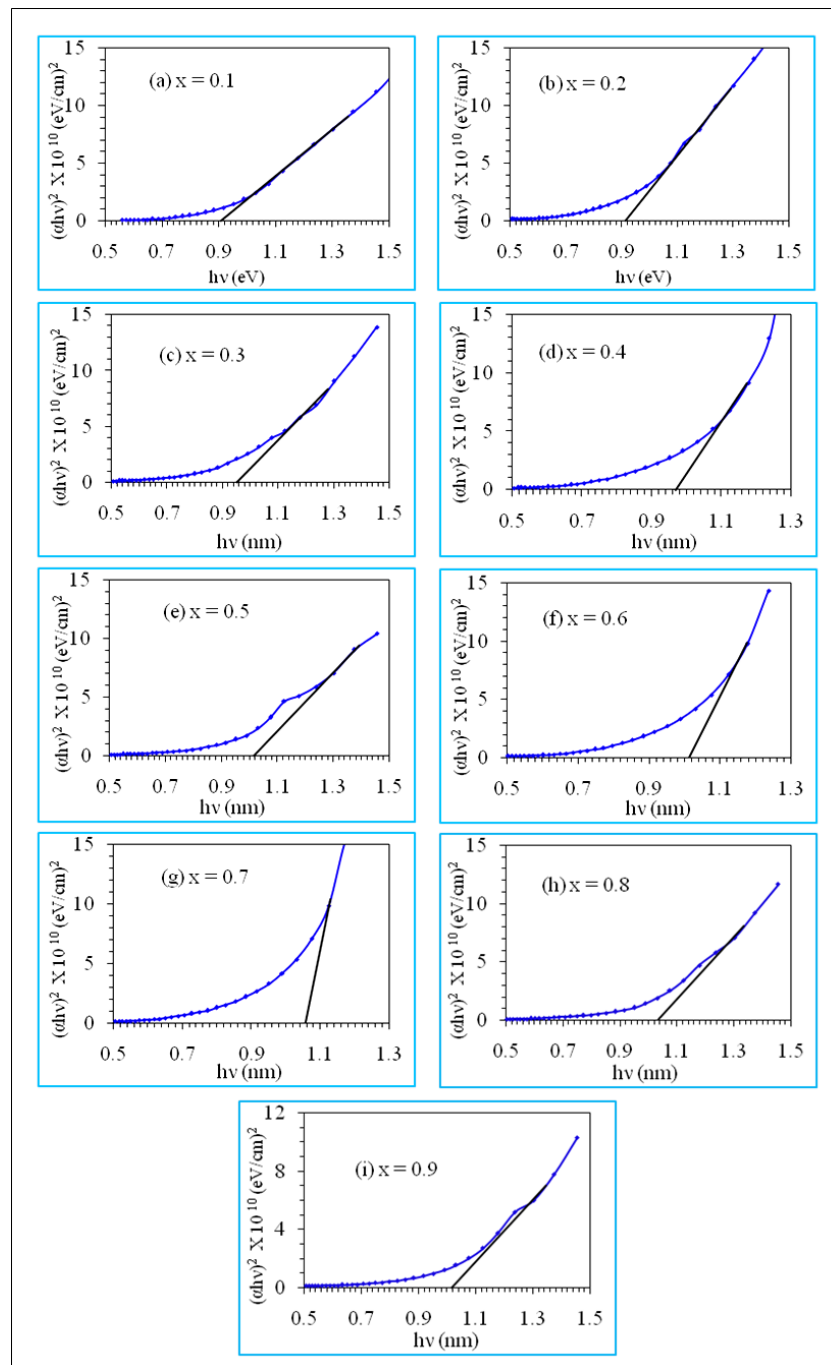


**Fig 5:** Variation of  $(\alpha h\nu)^2$  with photon energy ( $h\nu$ ) for annealed  $\text{Sb}_{2x}\text{Bi}_{2(1-x)}\text{Te}_3$  thin films

The variation of observed lattice parameter ( $a$ ) and band gap ( $E_g$ ) with composition ( $x$ ) is shown in Fig. 6.

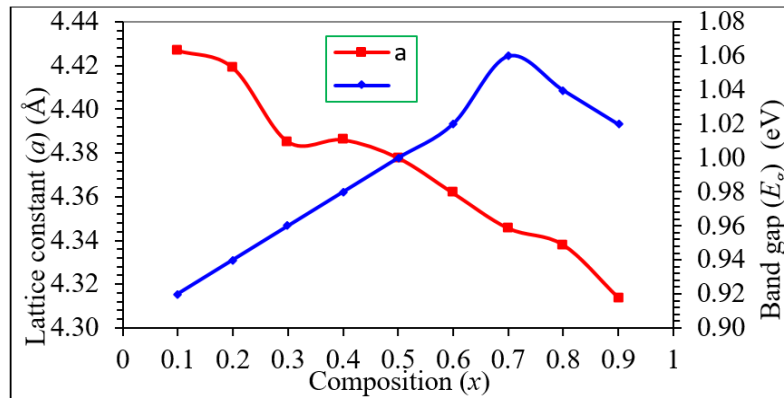


**Fig 6:** Variation of lattice constant ( $a$ ) and band gap ( $E_g$ ) with composition ‘ $x$ ’ for annealed  $Sb_{2x}Bi_{2(1-x)}Te_3$  thin films

Optical constants, refractive indices (n) and extinction coefficients (k) have been evaluated from the transmittance and reflectance data and using the following relations for normal incidence [15].

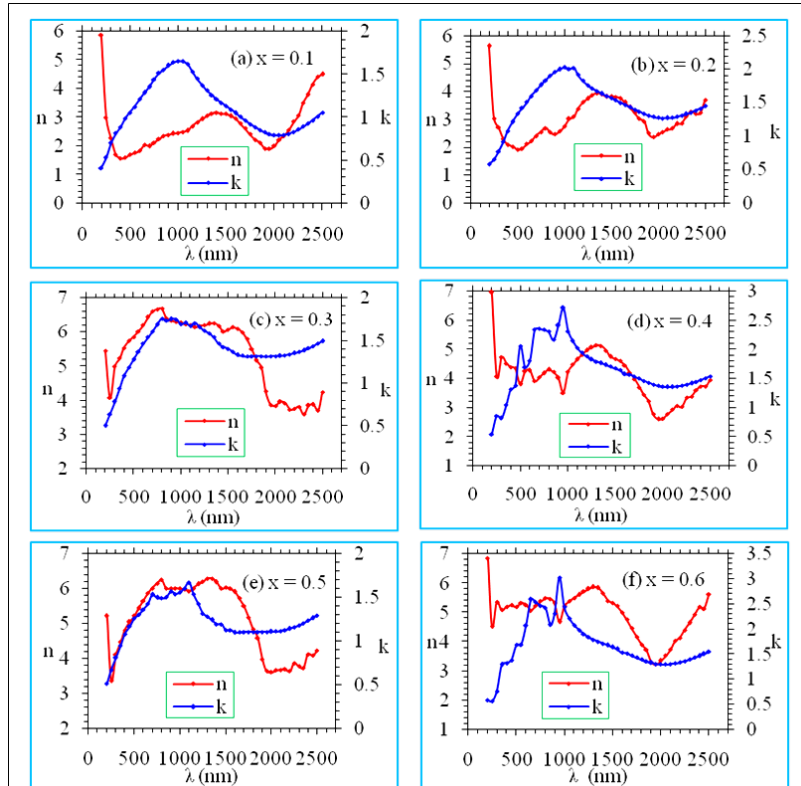
$$R = \frac{[(n-1)^2 + k^2]}{[(n+1)^2 + k^2]} \quad (3)$$

$$k = \frac{a\lambda}{4\pi} \quad (4)$$

The Fig. 7 (a) to (i) represents variation of refractive indices (n) and extinction coefficients (k) as a function of wavelength for the different compositions of  $Sb_{2x}Bi_{2(1-x)}Te_3$  thin films. As seen in Fig. 7, variations of ‘n’ and ‘k’ are rather oscillatory in nature, well-defined maxima and minima are observed as a function of wave length for different compositions of the films. The oscillations are enhanced for the compositions  $x =$

0.4 and 0.6.

The results from the curves in Fig. 7 shows that, for all the compositions ‘n’ is higher at  $\lambda = 200$  nm and then it decrease rapidly. The variations of ‘n’ are comparatively small in the spectral region 500-1700 nm. A refractive index minima is observed in the NIR region at wave length about 2000 nm. On the other hand extinction coefficient ‘k’ increases rapidly in the spectral region from 200 to 700 nm and shows maxima at wave length about 900 nm. The variations in ‘k’ are diminutive at higher wave lengths. For all compositions the extinction coefficient ‘k’ varies between 0.42 and 3.02, while refractive index ‘n’ varies between 1.58 and 8.42. Refractive index found to increase with increase in the composition. Extinction coefficient initially increases with increase in the composition then it decreases for the higher composition. Comparable results of the optical properties were reported by P. Barman *et al.* [16].



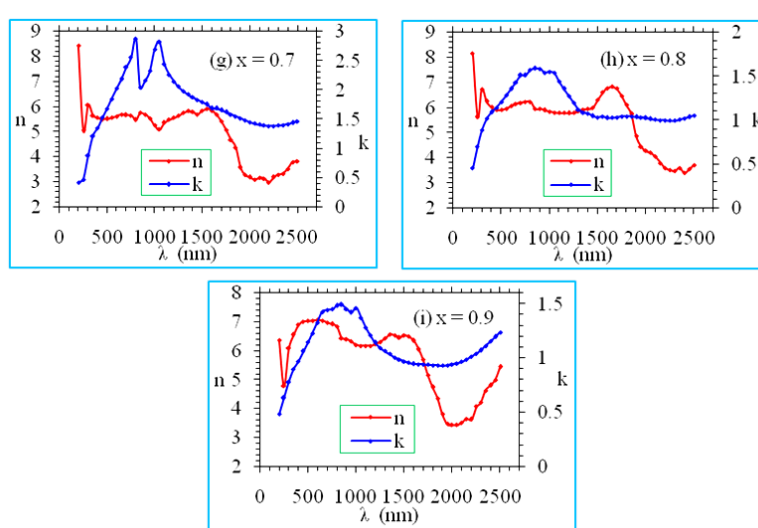


**Fig 7:** Variation of n and k with wavelength for annealed  $\text{Sb}_{2x}\text{Bi}_{2(1-x)}\text{Te}_3$  thin films

## Conclusions

The ternary thin films of  $\text{Sb}_{2x}\text{Bi}_{2(1-x)}\text{Te}_3$  of different compositions were deposited onto glass substrates by thermal evaporation and annealed at 473 K for 1 hour in vacuum. The XRD patterns show strong preferential orientation of the crystallites along (1010) direction for all the compositions. These samples also shows lower intensity peak for (110) and very low intensity peaks for (118) and (300) planes of hexagonal or rhombohedral phase corresponding to different compositions. The FESEM images show that the deposited films are polycrystalline in nature, closely packed with less inter grain spacing and uniform deposition. The grain size observed from FESEM images is about 20-60 nm, which is in good agreement with the XRD results. Optical transmittance spectra of the  $\text{Sb}_{2x}\text{Bi}_{2(1-x)}\text{Te}_3$  samples shows optical transparency in the spectral region between 1100 nm to 2500 nm, the transmittance falls steeply with decreasing wavelength and display a clear explicit absorption edge interrelated to the optical band gap depending on the composition of the films. The films with composition  $x = 0.1$  to 0.9 shows very distinct and well defined optical transmittance between 0% to 32%. The optical reflectance varies from 12% to 70 % and increases with increase in the composition. The optical band gap has been found to be direct and allowed. The band gap values vary between 0.92 eV to 1.06 eV with composition. Refractive index 'n' varies from 1.58 to 8.42 and extinction coefficient 'k' varies from 0.42 to 3.02 for all the compositions.

## Acknowledgements

I would like to express my sincere gratitude to my esteemed Research Guide, Prin. Dr. P. H. Pawar and Principal, Prof. Dr. G. B. Shelke for their priceless guidance, incessant support and reassurance throughout the course of this research work. Author is also thankful to the Chairman, Secretary and Management of the R. S. S. P. M. Ltd. Chalisgaon for their support at every step.

## References

- Zhou J *et al.* Manipulation of  $\text{Bi}^{3+}/\text{In}^{3+}$  Transmutation and  $\text{Mn}^{2+}$ -Doping Effect on the Structure and Optical Properties of Double Perovskite  $\text{Cs}_2\text{NaBi}_{1-x}\text{In}_x\text{Cl}_6$ . Advanced Optical Materials. 2019; 7(8).
- Zhou Q *et al.* Self-Powered Ultra-Broadband and Flexible Photodetectors Based on the Bismuth Films by Vapor Deposition. ACS Applied Electronic Materials. 2020; 2(5):1254.
- Manyk T *et al.* Method of electron affinity evaluation for the type-2 InAs/InAs $1-x$ Sbx superlattice. Journal of Materials Science. 2020; 55(12):5135.
- Noculak A *et al.* Bright Blue and Green Luminescence of Sb(III) in Double Perovskite  $\text{Cs}_2\text{MInCl}_6$  (M = Na, K) Matrices. Chemistry of Materials. 2020; 32(12):5118.
- Gilshtein E *et al.* Superstrate structured Sb\$-\$2\$S\$-\$3\$S\$ thin-film solar cells by magnetron sputtering of Sb and post-sulfurization, 2025.
- Stolzerm M, Stordeur M, Sobotta H, Riede V. Phys. Status. Solidi. B1. 1986; 138:259.
- Xiao Z, Zimmerman RL, Holland LR *et al.*, Nuclear Instruments and Methods in Physics Research Section B. 2006; 242:201-204.
- Singh AK. Opto-Electronics Review. 2012; 20(3):226-238.
- Jain N, Pancholi KC, Kakani SL. International Journal of Engineering Technology, Management and Applied Sciences. 2015; 3(2):219-226.
- Gupta S, Agarwal A, Saxena M. Adv. in Appl. Sci. Research. 2011; 2(4):49-57.
- Cullity BD. Elements of X-ray Diffraction, 2<sup>nd</sup> ed., Addison-Wesley Publishing Company, Massachusetts, USA, 1978.
- Rajasekar K, Subbarayan A, Sathyamoorthy R. Solar Energy Materials and Solar Cell. 2006; 90:2515-2522.
- Sharma K, Lal M, Gumber VK, Kumar A, Chaudary N, Goyal N. J. of Nano and Electronic Physics. 2014; 6(1):01007(6).
- Jain N, Kakani SL, Pancholi KC. International Journal for Scientific Research and Development. 2014; 2(9):93-95.
- Goswami A. Thin Film Fundamentals, New Age International Pvt. Ltd., 2014, 442.
- P. Barman and P. Sharma, Glass Physics and Chemistry. 2013; 39(3):276.